RHEUMATOLOGY

Rheumatology 2021;00:1–13
https://doi.org/10.1093/rheumatology/keab900
Advance access publication 3 December 2021

Original article

Perivascular and endomysial macrophages expressing VEGF and CXCL12 promote angiogenesis in anti-HMGCR immune-mediated necrotizing myopathy

Anna Lia[1,*], Tiziana Annese [2,*], Marco Fornaro[3,*], Margherita Giannini [3,4], Dario D'Abbicco[5], Mariella Errede[2], Loredana Lorusso [2], Angela Amati[1], Marilina Tampoia [6], Maria Trojano[1], Daniela Virgintino[2], Domenico Ribatti[2], Luigi Serlenga[1], Florenzo Iannone [3,*] and Francesco Girolamo[2]

Abstract

Objectives. To study the phenotype of macrophage infiltrates and their role in angiogenesis in different idiopathic inflammatory myopathies (IIMs).

Methods. The density and distribution of the subpopulations of macrophages subsets (M1, inducible nitric oxide$^+$, CD11c$^+$; M2, arginase-1$^+$), endomysial capillaries (CD31$^+$, FLK1$^+$), degenerating (C5b-9$^+$) and regenerating (NCAM$^+$) myofibres were investigated by immunohistochemistry in human muscle samples of diagnostic biopsies from a large cohort of untreated patients (*n*: 81) suffering from anti-3-hydroxy-3-methylglutaryl coenzyme A reductase (anti-HMGCR)$^+$ immune mediated necrotizing myopathy (IMNM), anti-signal recognition particle (anti-SRP)$^+$ IMNM, seronegative IMNM, DM, PM, PM with mitochondrial pathology, sporadic IBM, scleromyositis, and anti-synthetase syndrome. The samples were compared with mitochondrial myopathy and control muscle samples.

Results. Compared with the other IIMs and controls, endomysial capillary density (CD) was higher in anti-HMGCR$^+$ IMNM, where M1 and M2 macrophages, detected by confocal microscopy, infiltrated perivascular endomysium and expressed angiogenic molecules such as VEGF-A and CXCL12. These angiogenic macrophages were preferentially associated with CD31$^+$ FLK1$^+$ microvessels in anti-HMGCR$^+$ IMNM. The VEGF-A$^+$ M2 macrophage density was significantly correlated with CD (r_S: 0.98; *P*: 0.0004). Western blot analyses revealed increased expression levels of VEGF-A, FLK1, HIF-1α and CXCL12 in anti-HMGCR$^+$ IMNM. CD and expression levels of these angiogenic molecules were not increased in anti-SRP$^+$ and seronegative IMNM, offering additional, useful information for differential diagnosis among these IIM subtypes.

Conclusion. Our findings suggest that in IIMs, infiltrating macrophages and microvascular cells interactions play a pivotal role in coordinating myogenesis and angiogenesis. This reciprocal crosstalk seems to distinguish anti-HMGCR associated IMNM.

Key words: myositis, neovascularization, necrotizing myopathy, M2 macrophages

[1]Unit of Neurophysiopathology, [2]Unit of Human Anatomy and Histology, Department of Basic Medical Sciences, Neuroscience and Sense Organs, [3]Unit of Rheumatology, Department of Emergency and Organ Transplantation, University of Bari, Bari, Italy, [4]Service de Physiologie, Unité d'Explorations Fonctionnelles Musculaires, Hôpitaux Universitaires de Strasbourg, Strasbourg, France, [5]Institute of General Surgery 'G. Marinaccio', Department of Emergency and Organ Transplantation, University of Bari, Bari and [6]Unit of Clinical Pathology, Ospedale SS. Annunziata, Taranto, Italy

Submitted 12 August 2021; accepted 29 November 2021

Correspondence to: Girolamo Francesco, Sezione Anatomia Umana, Piazza Giulio Cesare, 11, 70124 Bari, Italy.
E-mail: francesco.girolamo@uniba.it

*These authors contributed equally to this study.

Rheumatology key messages

- The VEGF-A$^+$ CXCL12$^+$ angiogenic macrophages accumulated near CD31$^+$ FLK1$^+$ microvessels.
- In anti-HMGCR$^+$ immune-mediated necrotizing myopathy (IMNM), VEGF-A$^+$ M2 density correlated with capillary density, that was 2-fold the VEGF-A$^+$ M1 density.
- Anti-SRP and seronegative IMNM had few VEGF-A$^+$ CXCL12$^+$ angiogenic macrophages and capillary density was not increased.

BASIC SCIENCE

Introduction

Idiopathic inflammatory myopathies (IIMs) are a group of acquired immune-mediated diseases that share muscle weakness, inflammatory infiltrates, increased levels of creatine kinase (CK), variable involvement of other organs, and potentially effective therapies. Among IIMs, immune-mediated necrotizing myopathy (IMNM) has been pathologically characterized by a diffuse distribution of myofibres in different stages of degeneration and necrosis, together with regenerating myofibres [1, 2]. This phenotype has been associated with two myositis-specific autoantibodies, namely anti-signal recognition particle (anti-SRP) [3] and anti-3-hydroxy-3-methylglutaryl-coenzyme A reductase (anti-HMGCR) [4, 5]. Anti-SRP autoantibodies are present in 5–15% of IIM patients [6, 7], and anti-HMGCR autoantibodies in 6–10% [4, 6–8]. Although anti-SRP$^+$ myopathy is considered more severe than anti-HMGCR$^+$ IMNM [1, 7, 9], macrophages abundantly infiltrate muscle tissue, regardless of the autoantibody pattern. Furthermore, these macrophages appear localized both in the endomysial space, surrounding 'normal appearing' myofibres, and in perimysial and perivascular spaces [1]. These abundant inflammatory cells found in the IMNM specimens were related to the IMNM pathogenesis, together with autoantibodies-mediated complement deposition [1, 10]. At least two distinct, polarized subpopulations of macrophages have been described in IMNM muscles, namely inducible nitric oxide synthase-positive (iNOS$^+$) M1 pro-inflammatory macrophages and CD206$^+$ M2 regenerative macrophages, known to release pro-fibrotic molecules [1, 10–12]. The balance between the activity of these two macrophage subpopulations could be responsible for the different myopathological features observed in IMNM. M1 aggressive macrophages abundantly accumulated in both anti-HMGCR$^+$ and anti-SRP$^+$ IMNM [1, 13]. However, M2 reparative macrophages prevailed in anti-HMGCR$^+$ IMNM [10]. M2 macrophages are known to produce pro-healing factors via the secretion of VEGF, IL 10, and TGF-β in muscle regeneration models [14]. All these macrophage-derived molecules also induce a robust angiogenesis [15, 16]. VEGF is a selective endothelial mitogen that was shown to be overexpressed by myofibres in other IIMs, DM, PM and sporadic IBM [17–20].

Another angiogenic factor, C-X-C motif chemokine ligand 12 (CXCL12), shown to promote muscle regeneration and to counteract the progressive fibro-adipose tissue remodelling [21, 22], was immunolocalized in myofibres, blood vessels, T-helper lymphocytes and macrophages in DM, PM and sporadic IBM [23]. In IMNM patients, neither VEGF nor CXCL12 have yet been examined. In the present study, the distribution and density of M1/M2 macrophages producing these two angiogenic factors have been investigated by high-resolution confocal microscopy and western blot (WB) analyses. In addition, we searched for a possible correlation between pro-angiogenic macrophages and the densities of endomysial and perimysial vessels. This could provide further insights into the pathogenesis of different IMNMs.

Materials and methods

Single open biopsies of muscle tissue obtained for diagnostic purposes from 81 patients with clinically and pathologically confirmed IIMs were retrospectively reviewed. The presence of myositis-specific autoantibodies was determined in all patients by commercially available enzyme immunoassay (MYO12D-24, D-Tek, Mons, Belgium) that can detect autoantibodies against Jo-1, PL-7, PL-12, EJ, SRP, Mi-2, MDA-5, TIF1-gamma, HMGCR, SSA/Ro52, SAE-1/2 and NXP-2 antigens. Histopathology, immunohistochemical (IHC) and WB analyses were performed before the start of any treatment on muscle biopsies from eight patients with anti-HMGCR$^+$ IMNM (two patients exposed and six patients not exposed to statin), five patients with anti-SRP$^+$ IMNM, eight patients with seronegative IMNM (no myositis-specific autoantibodies nor myositis-associated autoantibodies). Additional muscle samples were taken from 21 patients with adult DM, eight patients with PM, eight patients with systemic sclerosis-overlap myositis (SSc-OM), eight patients with anti-synthetase syndrome (ASS, six Jo1$^+$ and two PL7$^+$), five patients with PM with mitochondrial pathology (PM-Mito), three patients with adult mitochondrial myopathy (MM), 10 patients with sporadic IBM and six age-matched healthy subjects, used as controls. The patients underwent a complete medical history, electromyography and nerve conduction studies, non-contrast bilateral thigh magnetic resonance imaging, pulmonary function tests, malignancy screening, laboratory evaluations, as previously described [24]. Specific diagnoses were made according to the defined criteria specified in Supplementary Methods, available at *Rheumatology* online. Normal control specimens were derived from apparently healthy subjects with mildly elevated serum CK levels, but without any histological abnormality, including the absence of inflammatory infiltrates or MHC class I up-regulation. All procedures performed in this study were in accordance with the ethical standards of the 1964 Helsinki Declaration and its later amendments. The study was reviewed and approved by the Medical Ethics Committee of the Regional Policlinico University Hospital of Bari (study no. 6229, approval no. 84762, 2020/11/06; comitatoetico@policlinico.ba.it). All patients gave signed informed consent to the diagnostic and research analyses and specimens inclusion in a muscle biobank.

The muscle biopsy specimens underwent standard histochemical and IHC staining, WB analyses and quantitative evaluations, as detailed in the Supplementary Methods, available at *Rheumatology* online.

Categorical variables were expressed as number or percentage; continuous variables as mean (S.D.). Comparisons between-groups were performed using parametric and non-parametric tests, as appropriate. T test and one-way ANOVA followed by Tukey's multiple comparison test were used to compare morphology data, while Kruskal–Wallis test followed by Dunn's multiple comparison test

were used to compare WB results. Differences were considered statistically significant when the *P*-value was ≤ 0.05. Spearman's rank-order correlation analysis was performed to identify interdependent variables. All statistical analyses were performed using GraphPad Prism (release 7.04, GraphPad Software, La Jolla, CA, USA).

Results

Demographic information, CK levels at muscle biopsy time, and other clinical features of IIM patients and age-matched controls are shown in Supplementary Table S1, available at *Rheumatology* online. None of the IIM patients had a family history of muscle disease. All patients are of Caucasian ethnicity and referred with muscle weakness lasting from 1 to 28 months before the biopsy. None of the 84 patients had cancer-associated myositis (3 years before/after the symptoms onset). The average age at disease diagnosis (baseline) and the gender distribution were both similar among the different groups (Supplementary Table S1, available at *Rheumatology* online). At baseline, no differences were found in physician assessments of the manual muscle test-8 items and in the disease severity on a 0–10 visual analogue scale. CK levels were higher in patients affected with IMNM, without reaching the statistical significance ($P > 0.05$) (Supplementary Table S1, available at *Rheumatology* online).

Systematic observation of the vascular network of different IIM diseases by IHC staining with the endothelial marker CD31 revealed a prominent capillary density (CD) in anti-HMGCR$^+$ IMNM, where numerous CD31$^+$ endothelial cells appeared hypertrophic and created an increased network of transverse and longitudinal endomysial microvessels (Fig. 1). To verify whether the vascular supply of affected skeletal muscles differs among different IIMs, several vascular parameters were measured using CD31 IHC. The endomysial CD31$^+$ CD was confirmed to be significantly increased in anti-HMGCR$^+$ IMNM compared with controls, DM, PM, SSc-OM, ASS and sporadic IBM specimens, but significantly lower than the highest calculated value of MM specimens (Table 1; Fig. 1). In addition, CD31$^+$ CD were lower in PM, SSc-OM and ASS than in seronegative IMNM and PM-Mito. In adult DM specimens, the CD of regions without perifascicular atrophic fibres was similar to controls, and this datum biased against possible statistical difference with controls (data not shown) [25]. In any case, the DM CD appeared significantly lower than MM and PM-Mito. As already described [25], the percentage area affected by capillary depletion appeared significantly higher in DM than in the other IIMs (Supplementary Table S1, available at *Rheumatology* online). The capillary to fibre ratio (C : F) was significantly lower in DM, PM, SSc-OM, ASS and sporadc IBM than in controls, MM, PM-Mito and IMNM (Table 1). The CD31$^+$ area percentage, the CD31 integrated density (the product of the stained area and mean grey value of positive pixels), the density of perimysial vessels and their diameters were all similar in different IIM groups compared with controls, but the percentage of perimysial vessels with a thickened wall, an aspect present in 13 of 21 (61.9%) adult DM patient biopsies, was significantly higher than in controls, PM, SSc-OM, ASS and anti-HMGCR$^+$ IMNM (Fig. 1; Supplementary Table S1, available at *Rheumatology* online).

An increased CD was disclosed in anti-HMGCR$^+$ IMNM, where distinct signs of muscle necrosis and regeneration coexisted, as previously described [1, 24]. Also in our study, a higher percentage of non-necrotic myofibres with sarcolemmal complement deposition was found in anti-HMGCR$^+$ IMNM than controls (Table 1), along with the highest density of NCAM$^+$ regenerating myofibres (Supplementary Table S1, available at *Rheumatology* online), even if this was not significantly different from the other IIMs. Moreover, the myofibre density was similar to controls in all IMNM subgroups, but increased in DM (Supplementary Table S1, available at *Rheumatology* online), due to perifascicular atrophic myofibres. In IMNM, the presence of an endomysial and perivascular inflammatory infiltrate, mainly composed of CD68$^+$ macrophages, was demonstrated (Fig. 2). Accordingly, a significantly higher CD68$^+$ macrophage density was found in anti-HMGCR$^+$ IMNM and in SSc-OM than in controls, whereas this density was relatively lower in anti-SRP$^+$ and seronegative than in anti-HMGCR$^+$ IMNM (Table 1, Fig. 2). In IMNM specimens, CD68$^+$ macrophages appeared preferentially located in proximity to CD31$^+$/FLK1$^+$ endomysial capillaries (Fig. 2e and f).

In the attempt to couple these signs of myogenesis and angiogenesis with the presence of inflammatory infiltrates, we next looked for the cellular source of established angiogenic factors. We found scattered CD68$^+$ macrophages colocalizing with the inducible subunit of the HIF-1α, a transcription factor known to regulate genes promoting vascularization (Fig. 2a and b). Weak HIF-1α staining was detected on myofibres (Fig. 2a and b). VEGF-A is the primary gene upregulated by HIF-1α, and it was also co-immunolocalized with CD68 in IMNM specimens (Fig. 2). Like HIF-1α, VEGF-A$^+$ myofibres and vessels were rarely detected in IMNM (Figs 2 and 3), but more often in DM specimens (VEGF-A$^+$ myofibres: IMNM 0.71 (0.89)%; DM 10.87 (6.37)%, predominantly perifascicular; $P < 0.0001$). To define the density of macrophages expressing VEGF-A and to investigate the prevalence of M1 or M2 subpopulations in IMNM [1, 10, 12], we performed a morphometric analysis of macrophage subpopulations using two specific M1 markers, iNOS and CD11c, and arginase-1 as a marker of M2 reparative macrophages. Firstly, iNOS$^+$/CD11c$^+$ M1 toxic macrophages were scattered distributed in 87.5% anti-HMGCR$^+$, all anti-SRP$^+$ and seronegative IMNM; the density of M1 macrophages was significantly higher in anti-HMGCR$^+$ and anti-SRP$^+$ IMNM than controls, but similar in these two IMNM subgroups (Table 1; Fig. 3). Instead, all IMNM biopsies showed a scattered endomysial distribution of arginase-1$^+$ M2 reparative macrophages, although the density of

Fig. 1 Capillary density is increased in anti-HMGCR$^+$ IMNM and mitochondrial myopathy

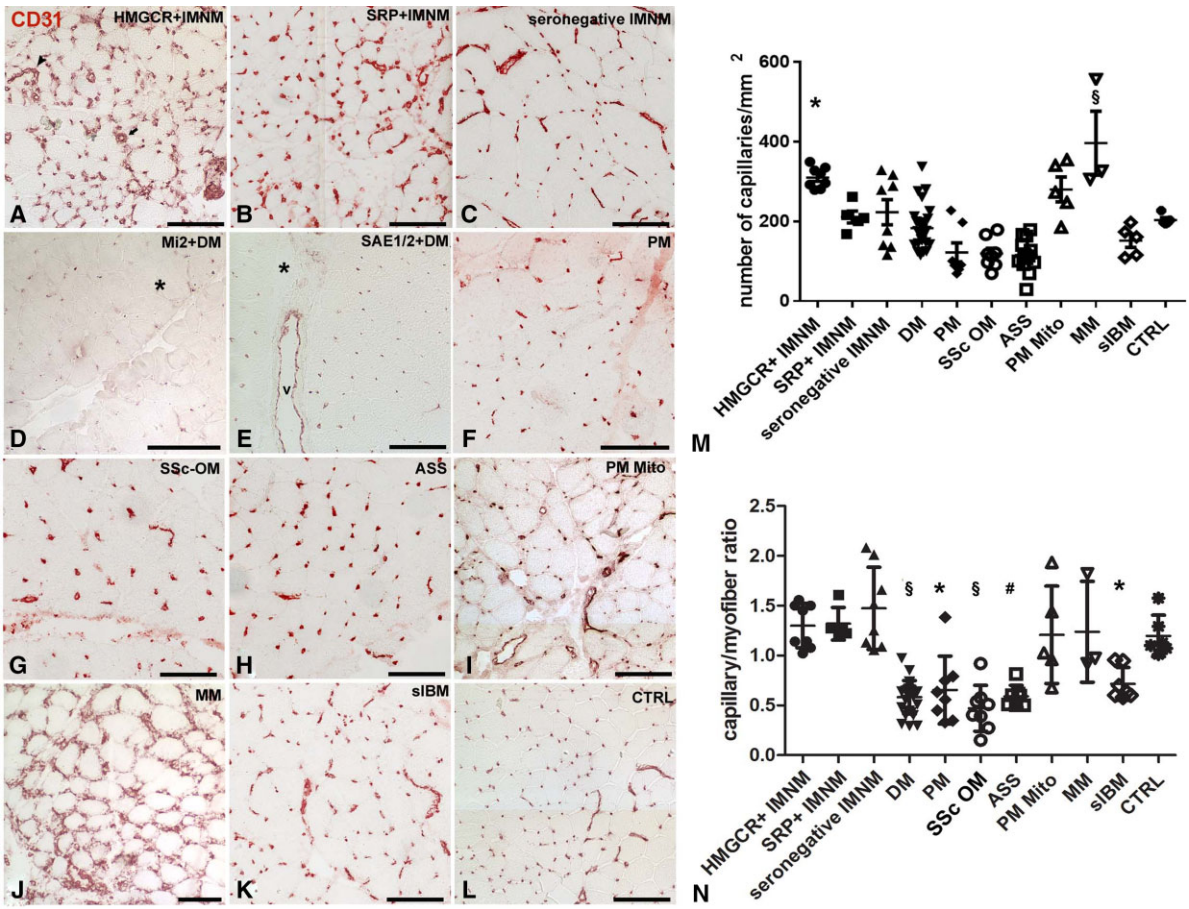

Representative light microscopy images (**A–L**) showing the muscle vessel network visualized by means of CD31 immunostaining in the different pathological muscle conditions and in control specimens. In anti-HMGCR$^+$ IMNM (**A**), an increased network of endomysial capillaries is evident, and CD31$^+$ endothelial cells appear hypertrophic in both transverse (arrow) and longitudinal sections (arrowhead). In anti-Mi2$^+$ (**D**) and anti-SAE1/2$^+$ (**E**) DM, the capillary network appears depleted, especially in perifascicular regions (asterisks) where the wall of a perimysial vessel (v) appears thickened. In MM (**J**), an exceptionally increased network is also visible. (**M**) Quantification of capillary density (number of endomysial blood microvessels/mm^2 of muscle tissue) shows an increased number in anti-HMGCR$^+$ IMNM and MM compared with controls. (**N**) The ratio between the amount of capillaries/amount of myofibres is significantly reduced in DM, PM, SSc-OM, ASS and sporadic IBM. Scale bars: 150 μm. One-way ANOVA test with Tukey's comparison was applied. *$P \leq 0.05$, #$P \leq 0.01$, §$P \leq 0.001$ for the comparison with control (CTRL) muscle. IMNM: immune-mediated necrotizing myopathy; MM: mitochondrial myopathy.

M2 macrophages was significantly higher than in controls and the other myopathies analysed only in anti-HMGCR$^+$ IMNM (Table 1). Most of the M1 and M2 macrophages with triangular shapes or elongated cytoplasmic processes were distributed near endomysial capillaries or in close contact with myofibres (Figs 2 and 3). Quantification of the ratio between M1 and M2 macrophage densities showed a predominance of M1 toxic macrophages in anti-SRP and seronegative IMNM, DM and sporadic IBM, but without any significant difference from controls (Table 1).

The analysis of triple immunolabelled muscle sections with anti-VEGF-A, anti-CD11c, anti-iNOS or anti-arginase-1 antibodies showed an endomysial accumulation of VEGF-A$^+$ macrophages in both M1 and M2 subpopulations. The calculated densities of VEGF-A$^+$/iNOS$^+$/CD11c$^+$ M1 toxic and VEGF-A$^+$/arginase-1$^+$ M2 reparative macrophages were significantly higher in anti-HMGCR$^+$ IMNM than the other IIMs and controls (Table 1, Fig. 3A–D). In addition, a fair proportion [27.83 (24.27)%] of arginase-1$^+$ macrophages also expressed low levels of CD11c, showing the presence in the IMNM subgroups of an intermediate CD11c^{low}/arginase-1^{high} M2 phenotype of macrophages expressing VEGF-A, probably stemming from the M1 subpopulation (Fig. 3B and D).

A positive correlation was observed in anti-HMGCR$^+$ IMNM between the endomysial CD31$^+$ CD and the

Table 1 Vascular and inflammatory cells morphometric parameters in idiopathic inflammatory myopathies.

Myopathy disease group Parameter	Anti-HMGCR immune mediated necrotizing myopathy (HMGCR)	Anti-SRP immune mediated necrotizing myopathy (SRP)	Seronegative immune mediated necrotizing myopathy (seroneg.)	Adult DM	PM	Overlap Myositis with systemic sclerosis (SSc-OM)	Anti-synthetase myositis (ASS)	PM with mitochondrial pathology (PM-Mito)	Mitochondrial myopathy (MM)	Sporadic IBM	Age-matched controls
Number of patients per disease group	8	5	8	21	8	8	8	5	3	10	6
Endomysial CD31^{+} capillary density[a,b]	303.18 (27.19)[d-j]	210.04 (38.47)[j]	223.24 (89.47)[j]	183.49 (52.18)[j,n]	122.39 (63.09)[j,n,p]	119.4 (36.23)[j,n,p]	127.76 (29.41)[j,n,p]	280.43 (69.52)[f,j,o]	456.85 (76.4)[r,t]	151.61 (37.92)[j]	203.93 (13.38)[j]
Capillary/myofiber ratio[a]	1.24 (0.22)	1.36 (0.2)	1.47 (0.41)	0.57 (0.16)[d,j,n,p-r]	0.68 (0.35)[d,j,n,p-r]	0.47 (0.23)[d,j,n,p-r]	0.63 (0.12)[d,j,n,p-r]	1.21 (0.32)	1.82 (0.69)	0.76 (0.17)[d,j,p-r]	1.21 (0.22)
% of myofibers with sarcolemmal C5b-9 staining[a]	1.34 (0.63)[d,f-i,n,s]	1.66 (0. 68)[d,f-i,n,s]	0.65 (0.93)	0.46 (0.81)	0.11 (0.21)	0.19 (0.35)	0.02 (0.06)	0.08 (0.17)	0.0 (0.0)	0.04 (0.1)	0.0 (0.0)
CD68^{+} density[a,b]	98.32 (37.92)[d,m]	25.24 (9.56)	32.14 (19.4)	37.09 (51.47)	32.51 (48.07)	84.48 (55.35)[d,m]	5.62 (9.25)	36.39 (37.12)	10.35 (17.02)	38.43 (73.99)	0.35 (0.87)
Density of iNOS^{+}/CD11c^{+} M1 toxic macrophages[a,b]	23.69 (14.03)[e-i,n,p,t]	16.28 (5.46)[m,t]	9.52 (6.56)	6.35 (5.01)	5.76 (4.82)	4.78 (5.45)	0.61 (1.23)	6.36 (4.89)	N.D.[c]	7.82 (2.56)	0.0 (0.0)
Density of arginase-1^{+} M2 reparative macrophages[a,b]	19.51 (4.81)[e-i,n,p,q,t]	3.36 (1.04)	1.5 (0.56)	4.08 (3.89)	3.46 (4.1)	2.34 (2.67)	4.93 (2.34)	2.35 (2.17)	N.D.[c]	1.89 (2.86)	0.0 (0.0)
Ratio of iNOS^{+} M1 macrophages to arginase-1^{+} M2 reparative macrophages[a]	1.38 (1.02)	5.18 (0.82)	6.85 (4.32)	5.41 (8.95)	1.68 (1.14)	2.57 (0.91)	0.28 (1.23)	2.71 (1.24)	N.D.[c]	4.25 (2.19)	0.03 (0.04)
Density of VEGF-A^{+}/iNOS^{+}/CD11c^{+} M1 toxic macrophages[a,b]	6.23 (3.94)[e,h,j,l,n,p,t-v]	2.46 (2.7)	1.98 (1.87)	1.99 (1.73)	3.1 (1.1)	2.66 (1.12)	1.2 (1.1)	1.49 (1.3)	N.D.[c]	1.4 (1.9)	0.0 (0.0)
Density of VEGF-A $^{+}$/arginase-1^{+} M2 reparative macrophages[a,b]	15.74 (2.01)[e-i,n,p,q,t]	3.18 (1.83)	2.76 (1.22)	1.61 (1.94)	1.2 (1.45)	1.68 (1.21)	0.56 (1.58)	0.56 (1.29)	N.D.[c]	1.38 (1.94)	0.0 (0.0)
Density of CXCL12^{+}/iNOS^{+} M1 toxic macrophages[a,b]	6.41 (3.08)[d,m]	5.74 (2.51)	4.79 (3.01)	3.48 (4.76)	2.61 (1.85)	1.56 (1.12)	0.0 (0.0)	3.56 (0.28)	N.D.[c]	1.98 (0.58)	0.0 (0.0)
Density of CXCL12^{+}/arginase-1^{+} M2 reparative macrophages[a,b]	3.47 (1.53)[f-h,t]	2.18 (1.22)[d]	1.95 (1.51)[d]	0.81 (0.19)	0.54 (0.26)	0.67 (0.48)	0.12 (0.24)	1.85 (0.59)	N.D.[c]	1.93 (0.86)	0.0 (0.0)

[a]mean (standard deviation);

[b]density: mean number of counted elements per biopsy area of 1 mm^{2} (standard deviation);

[c]N.D.: not determined.

By using Tukey's multiple comparison test:

[d]significantly different from control values at $p<<0.05$;

[e]significantly different from DM values at $p<0.0001$;

[f]significantly different from PM values at $p<0.001$;

[g]significantly different from SSc-OM values at $p<0.001$;

[h]significantly different from ASS values at $p<0.001$;

[i]significantly different from sIBM values at $p<0.001$;

[j]significantly different from MM values at $p<0.0001$;

[k]significantly different from PM values at $p<0.01$;

[l]significantly different from SSc-OM values at $p<0.01$;

[m]significantly different from ASS values at $p<0.01$;

[n]significantly different from PM-Mito values at $p<0.05$;

[o]significantly different from sIBM values at $p<0.05$;

[p]significantly different from seronegative values at $p<0.001$;

[q]significantly different from anti-SRP IMNM^{+} values at $p<0.0001$;

[r]significantly different from anti-HMGCR^{+} IMNM values at $p<0.0001$;

[s]significantly different from DM values at $p<0.05$;

[t]significantly different from control values at $p<0.001$;

[u]significantly different from anti-SRP IMNM^{+} values at $p<0.05$;

[v]significantly different from anti- SSc-OM $^{+}$ values at $p<0.05$.

Fig. 2 Endomysial macrophages express HIF-1α and VEGF-A while endothelial cells and *bona fide* endothelial precursors express FLK1

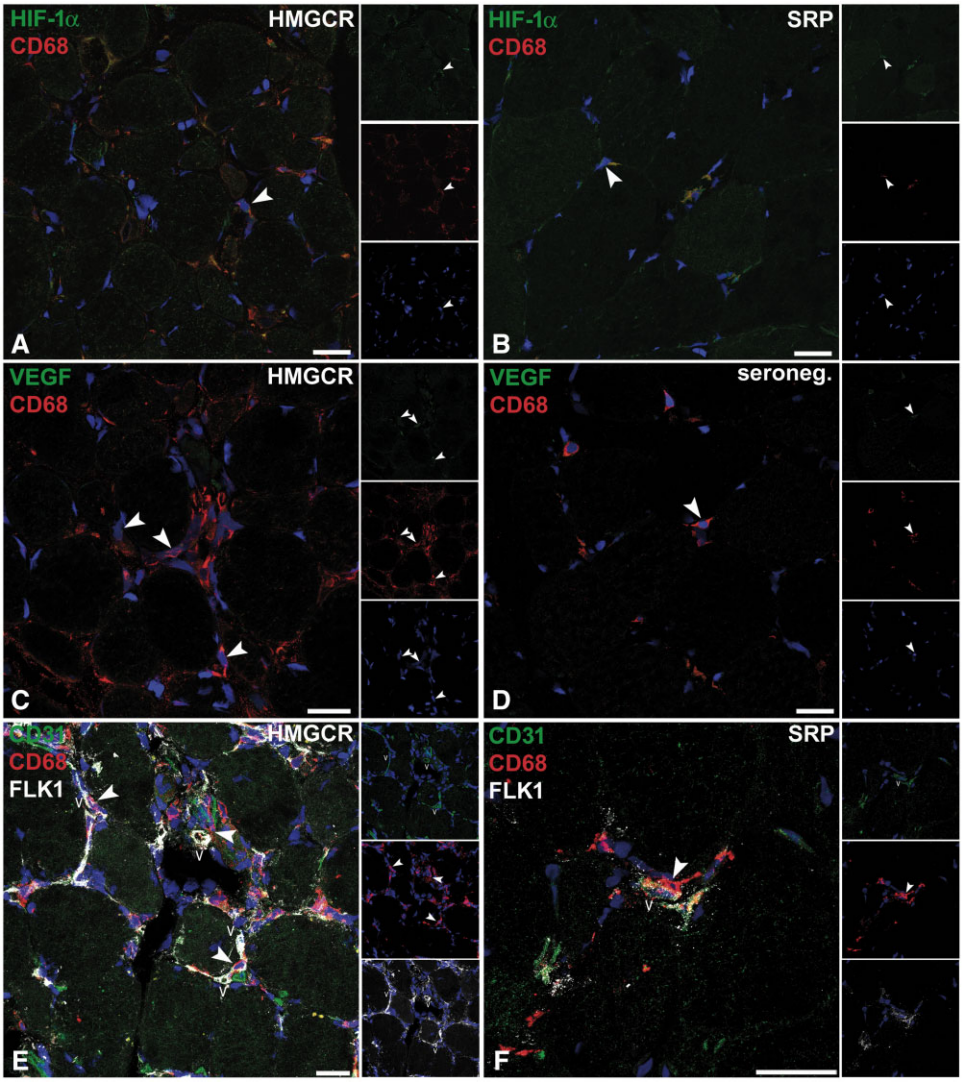

(**A–D**) Representative confocal microscopy images (enlarged overlay projections and miniatures for separate channels) showing double-positive (arrowheads) HIF-1α$^+$/CD68$^+$ (**A**, **B**) and VEGF-A$^+$/CD68$^+$ (**C**, **D**) macrophages in anti-HMGCR$^+$ (**A**, **C**), anti-SRP$^+$ (**B**), and seronegative (**D**) IMNM patients. Several skeletal muscle fibres express low levels of HIF-1α (**A**, **B**) and VEGF-A (**C**, **D**) in IMNM. (**E**, **F**) Representative confocal microscopy images of the preferential perivascular localization of CD68$^+$ macrophages (arrowheads) near CD31$^+$/FLK1$^+$ endomysial microvessels (v) in anti-HMGCR$^+$ (**E**) and anti-SRP$^+$ (**F**) IMNM muscle specimens. Scale bars: 25 μm. IMNM: immune-mediated necrotizing myopathy

VEGF-A$^+$/arginase-1$^+$ M2 density (r_S: 0.98; *P*: 0.0004), but neither with the total M1 and M2 densities, nor with the specific VEGF-A$^+$/iNOS$^+$/CD11c$^+$ M1 density (Fig. 3E). Other significant positive correlations were demonstrated between the CD and the M2 density in the IMNM subgroups (r_S: 0.56; *P*: 0.0072), the highest values being observed in anti-HMGCR$^+$ IMNM (Fig. 3F).

Another crucial angiogenic gene upregulated by HIF-1α, CXCL12, whose indirect activity increases VEGF-A synthesis, was investigated in IIMs (Fig. 4). Unexpectedly, VEGF-A and CXCL12 appeared co-expressed in scattered iNOS$^+$ M1 macrophages (Fig. 4C) and arginase-1$^+$ M2 macrophages (Fig. 4D and E). Quantification of the percentage of VEGF-A$^+$/CXCL12$^+$/iNOS$^+$ M1 toxic macrophages in the IMNM subgroups revealed that 3.13 (1.41)% of iNOS$^+$ M1 macrophages co-expressed VEGF-A and CXCL12, with significant differences between anti-HMGCR$^+$ [3.59 (1.32)%] and anti-SRP$^+$ [1.09 (0.14), $P = 0.0084$], but not seronegative ([2.84 (1.201), $P = 0.48$] IMNM. The proportion of arginase-1$^+$ M2 macrophages co-expressing VEGF-A and CXCL12 was even higher than

FIG. 3 Endomysial M1 and M2 macrophages both express VEGF-A in immune-mediated necrotizing myopathy

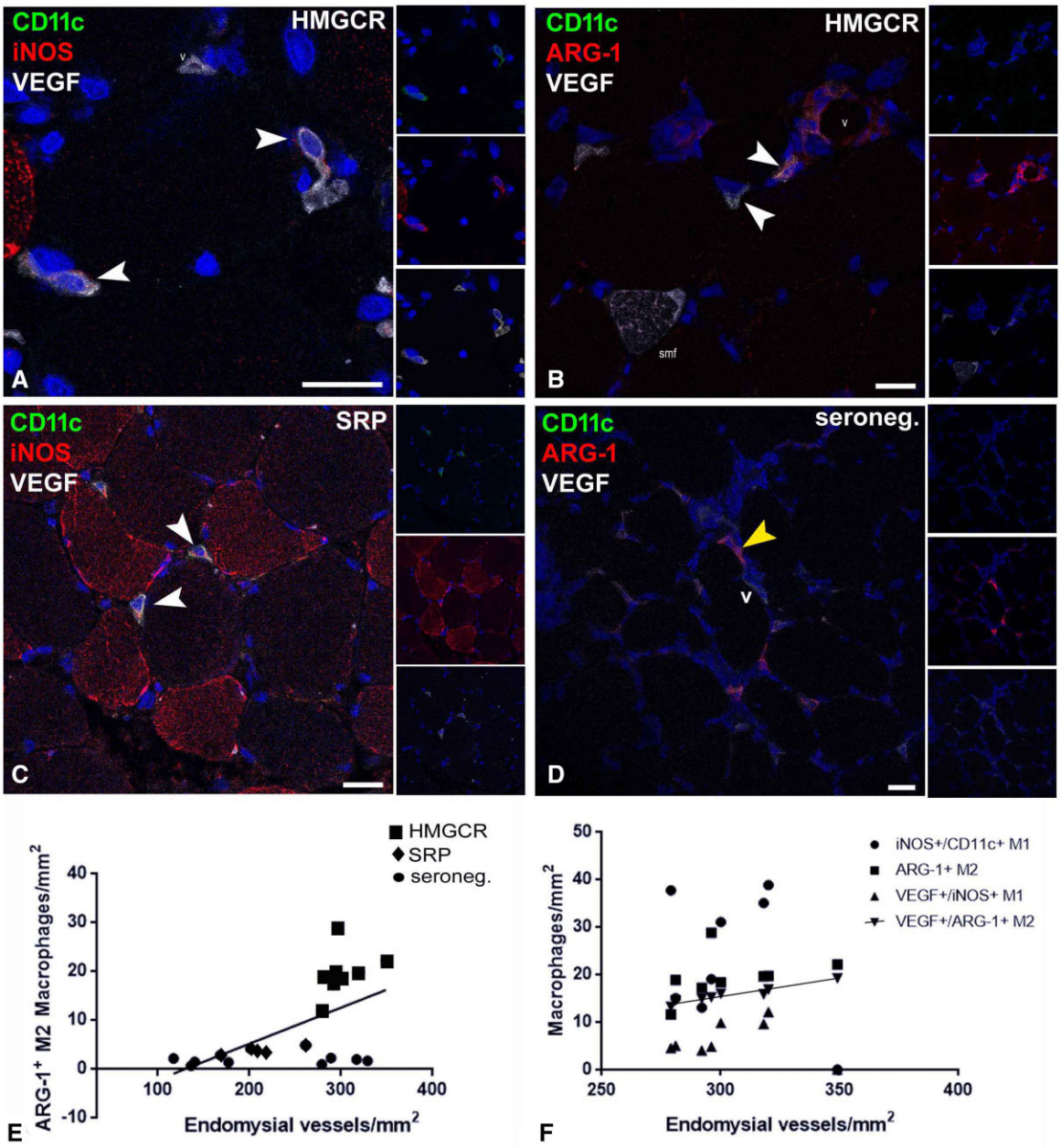

(**A–D**) Representative confocal microscopy images (enlarged overlay projections and miniatures for separate channels) showing triple positive (white arrowheads) iNOS$^+$/CD11c$^+$/VEGF$^+$ M1 macrophages (**A**, **C**) and arginase-1$^+$/CD11c$^+$/VEGF-A$^+$ M2 macrophages (**B**, **D**) in anti-HMGCR$^+$ (**A**, **B**), anti-SRP$^+$ (**C**), and seronegative (**D**) IMNM patients. Several skeletal muscle fibres express iNOS in IMNM (**A**, **C**), whereas additional VEGF-A is preferentially expressed by endothelial cells of blood vessels (v) and skeletal muscle fibres (smf) in anti-HMGCR$^+$ IMNM patients (**A**, **B**). VEGF-A-expressing macrophages are less frequently observed in seronegative than anti-HMGCR$^+$ IMNM, where VEGF-A-negative macrophages [yellow arrowhead in (**D**)] and VEGF-A-positive endomysial microvessels (v) are present. (**E**) There is a significant correlation (r_S: 0.56; *P*: 0.0072) between individual densities of arginase-1$^+$ M2 macrophages and the capillary density (CD) values calculated for each muscle specimen from IMNM patients. The highest values are observed in anti-HMGCR$^+$ IMNM patients. (**F**) The densities of iNOS$^+$/CD11c$^+$ M1, arginase-1$^+$ M2, and their VEGF-A$^+$ M1 and M2 macrophage subpopulations are plotted for anti-HMGCR$^+$ IMNM patients in correlation with their individual CD. Only the density of VEGF-A$^+$ arginase-1$^+$ M2 macrophages is positively correlated with CD (r_S: 0.98; *P*: 0.0004). Scale bars: 25 μm. IMNM: immune-mediated necrotizing myopathy.

the M1 proportion in anti-HMGCR$^+$ [8.89 (8.38)%] when compared with anti-SRP$^+$ [1.2 (0.67), $P = 0.049$] and seronegative [1.91 (0.89), $P = 0.041$] IMNM. Consequently, the density of CXCL12$^+$/iNOS$^+$ M1 macrophages was significantly higher in anti-HMGCR$^+$ IMNM than controls and ASS, where these cells were not found (Table 1). Similarly, the density of CXCL12$^+$/arginase-1$^+$ M2 macrophages was higher in anti-HMGCR$^+$ IMNM than controls, PM, SSc-OM and ASS (Table 1). CXCL12 was also found in blood vessels and scattered hypotrophic myofibres in all IIM muscle specimens (Fig. 4), and its cognate receptor CXCR7 was localized on endothelial cells of endomysial capillaries and few CD11c$^+$ macrophages (Fig. 4A).

To confirm the morphological results, WB analyses (Fig. 5) were carried out on muscle specimens of the same patients. An increased expression of FLK1 was revealed in anti-HMGCR$^+$ IMNM, DM, ASS, PM-Mito and MM compared with controls (Fig. 5B; Supplementary Fig. S1, available at *Rheumatology* online). The total amount of VEGF-A was likewise significantly higher in anti-HMGCR$^+$ IMNM, ASS, PM-Mito, MM and sporadic IBM than controls (Fig. 5D; Supplementary Fig. S3, available at *Rheumatology* online). CXCL12 was significantly overexpressed in anti-HMGCR$^+$ IMNM, DM and ASS (Fig. 5E; Supplementary Fig. S4, available at *Rheumatology* online). Total HIF-1α was increased in anti-HMGCR$^+$ IMNM, ASS, PM-Mito, MM and sporadic IBM compared with controls (Fig. 5C; Supplementary Fig. S2, available at *Rheumatology* online). In anti-SRP$^+$ and seronegative IMNM, the levels of VEGF-A, HIF-1α, CXCL12 and especially of FLK1, were lower than in anti-HMGCR$^+$ IMNM (Fig. 5). Furthermore, although there was considerable variability between individual PM specimens, the results did not differ significantly from controls (Fig. 5).

Discussion

In this study employing IHC microscopy we found, for the first time, a significantly increased endomysial CD31$^+$ CD in anti-HMGCR$^+$ IMNM, and concomitantly, abundant endomysial and perivascular macrophages expressing two angiogenic molecules, VEGF-A and CXCL12.

Many studies have explored muscle vascular supply in several IIMs, especially in DM, PM, sporadic IBM, but also in SSc-OM and anti-SRP$^+$ IMNM [18, 26–30], demonstrating narrowed vessel lumina and reduced capillary networks [31, 32]. Nevertheless, the CD and C : F have not been previously studied in muscle specimens derived from the other IMNM subgroups and PM-Mito. IMNM is a relatively recent diagnostic category, mainly derived from the better characterization of PM patients [2]. The blood vessels of the firstly described anti-HMGCR$^+$ IMNM patients appeared abnormally enlarged (with no CD reduction in 5/8 patients), suggesting a microvasculopathy or dysfunctional angiogenesis [5]. Our comparative data on CDs in IIMs are in overall agreement with previously published data on DM, sporadic IBM, SSc-OM and MM [26, 27, 29–31, 33] with the notable exception of PM specimens, which were collectively described as having a higher CD than controls [26, 27, 30]. Previous descriptions of CD in PM patients are in contrast with our measurements (Table 1), probably owing to the heterogeneity of the PM group before the subtraction of the IMNM subgroups from the formerly heterogeneous clinical category defined as PM [2]. In this manuscript, we highlight the finding that a higher CD31$^+$ CD is a histological parameter that differentiates anti-HMGCR$^+$ IMNM from PM, SSc-OM, ASS and sporadic IBM, all characterized by the presence of degenerating/regenerating myofibres, but a reduced CD. Despite the rarity of PM-Mito histopathological features and hence limited number of patients in our study, the CD31$^+$ CD of PM-Mito appeared different from that of PM and sporadic IBM, further supporting differential diagnosis among these overlapping myositides.

In the myology context, the most reliable and commonly used parameter for studying vessel density is the C : F. However, our measures of C : F confirmed previous results obtained in DM, PM and MM [27, 33] and extended to the IMNM subgroups, SSc-OM, ASS and PM-Mito, providing useful information for differential diagnosis. A reduced C : F characterized DM, PM, SSc-OM, ASS and sporadic IBM, whereas IMNM subgroups, PM-Mito and MM showed comparable values to the normal C : F (Table 1).

The precise regulatory mechanisms of muscle capillary growth and CD are incompletely understood but are presumably associated with the habitual levels of physical activity involved in lowering local oxygen tension by promoting HIF-related gene expression to increase angiogenesis and oxygen supply. In our patient cohort, we included diagnostic muscle biopsies derived from drug-naïve IIM patients with a moderate to severe impairment of physical activity, including walking. Despite their low muscle activity, caused by worsening weakness during the days preceding the biopsy procedure, anti-HMGCR$^+$ IMNM and MM patients showed an increased CD, probably the effect of angiogenic stimuli independent of exercise-related hypoxia. The best-known regulator of angiogenesis is VEGF, whose expression is enriched in endomysial vessels of MM patients due to an alternative angiogenic mechanism independent of hypoxia [33]. Accordingly, we observed the highest CD levels in our MM patients, together with the highest HIF-1α, VEGF-A and FLK1 protein expression in their muscle tissue. Anti-HMGCR$^+$ IMNM, ASS and DM also showed an overexpression of these angiogenic molecules. In DM, it is not surprising to observe an overexpression of angiogenic [17, 19, 20, 23, 30] and anti-angiogenic factors [18, 34], due to thrombotic perimysial angiopathy. In ASS, too, an aborted angiogenic status, characterized by low CD and C : F and high angiogenic levels could be predictable considering the general hypoxic condition determined by the contemporary interstitial lung disease. A presumable anti-angiogenic mechanism, based on antibody interference with the angiogenic activity of the secreted threonyl-tRNA synthetase may be postulated at least for anti PL7$^+$ ASS

Fig. 4 Endomysial M1 and M2 macrophages both express CXCL12 in immune-mediated necrotizing myopathy

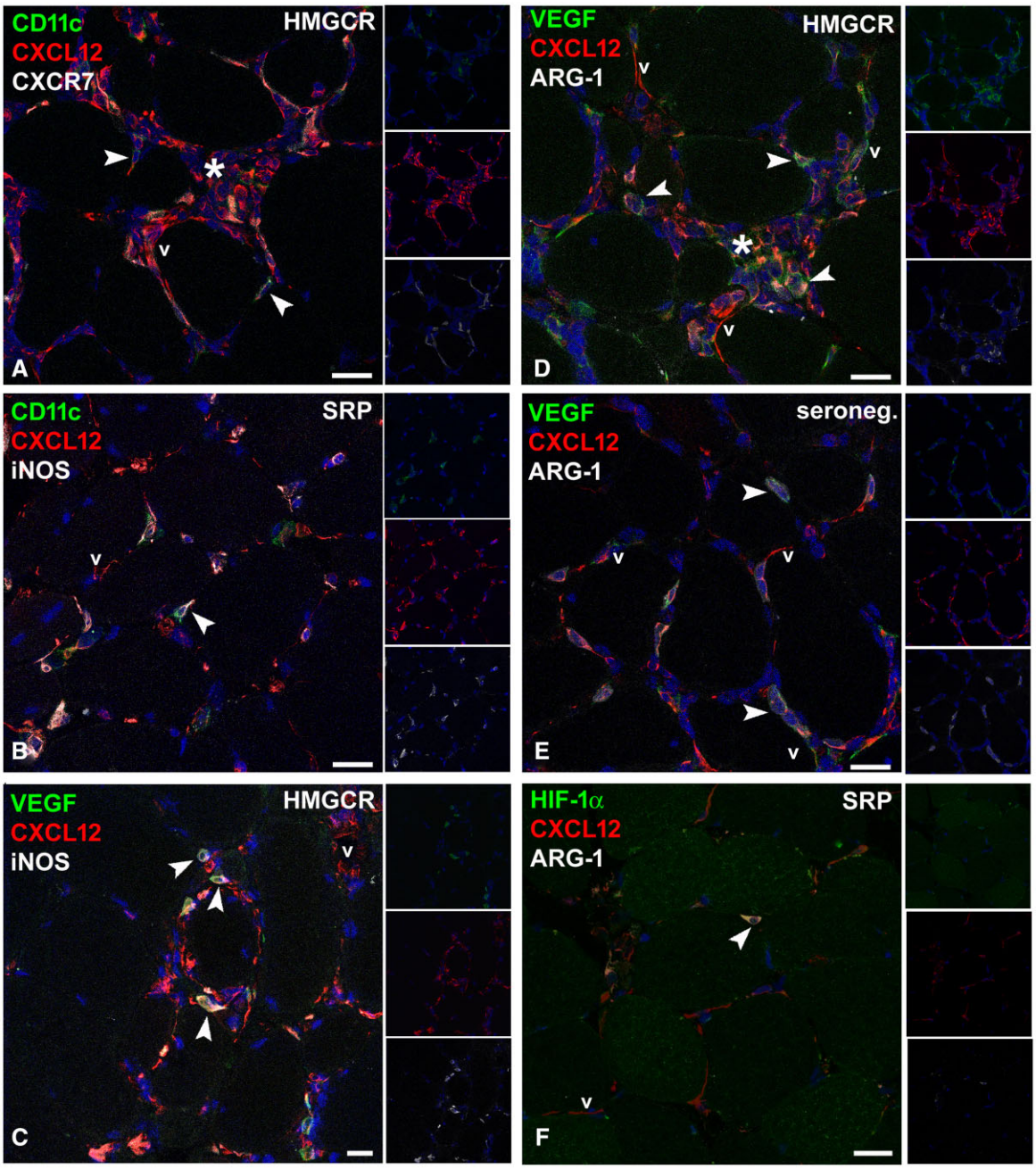

(**A–F**) Representative confocal microscopy images (enlarged overlay projections and miniatures for separate channels) showing triple positive (arrowheads) CXCR7$^+$/CD11c$^+$/CXCL12$^+$ (**A**), iNOS$^+$/CD11c$^+$/CXCL12$^+$ (**B**), VEGF-A$^+$/iNOS$^+$/CXCL12$^+$ (**C**) M1 macrophages, VEGF-A$^+$/arginase-1$^+$/CXCL12$^+$ (**D**, **E**) and HIF-1α^+/arginase-1$^+$/CXCL12$^+$ (**F**) M2 macrophages and CXCL12$^+$ VEGF-A$^+$ endomysial microvessels (v) in anti-HMGCR$^+$ (**A**, **C**, **D**), anti-SRP (**B**, **F**), and seronegative (**E**) IMNM patients. (**A**, **B**) The same inflammatory infiltrate of an anti-HMGCR$^+$ IMNM muscle specimen (asterisks) contains few distinguishable M1 (CD11c$^+$) and numerous M2 (ARG-1$^+$) macrophages; both subpopulations co-express CXCL12. Additionally, both M1 and M2 subpopulations also express VEGF-A in conjunction with CXCL12 (**C–E**; arrowheads). CXCL12 and its receptor CXCR7 are mainly immunolocalized in endomysial microvessel (v), but a lower level of expression is also visible in macrophages (arrowheads). (**F**) Very rarely the transcription factor HIF-1α is immunolocalized in arginase-1$^+$/CXCL12$^+$ M2 macrophages in IMNM patients. Note the abundant HIF-1α immunolabelling of myofibres in (**F**). Scale bars: 25 μm. IMNM: immune-mediated necrotizing myopathy.

Fig. 5 Classical molecular regulators of angiogenesis are increased in anti-HMGCR immune-mediated necrotizing myopathy

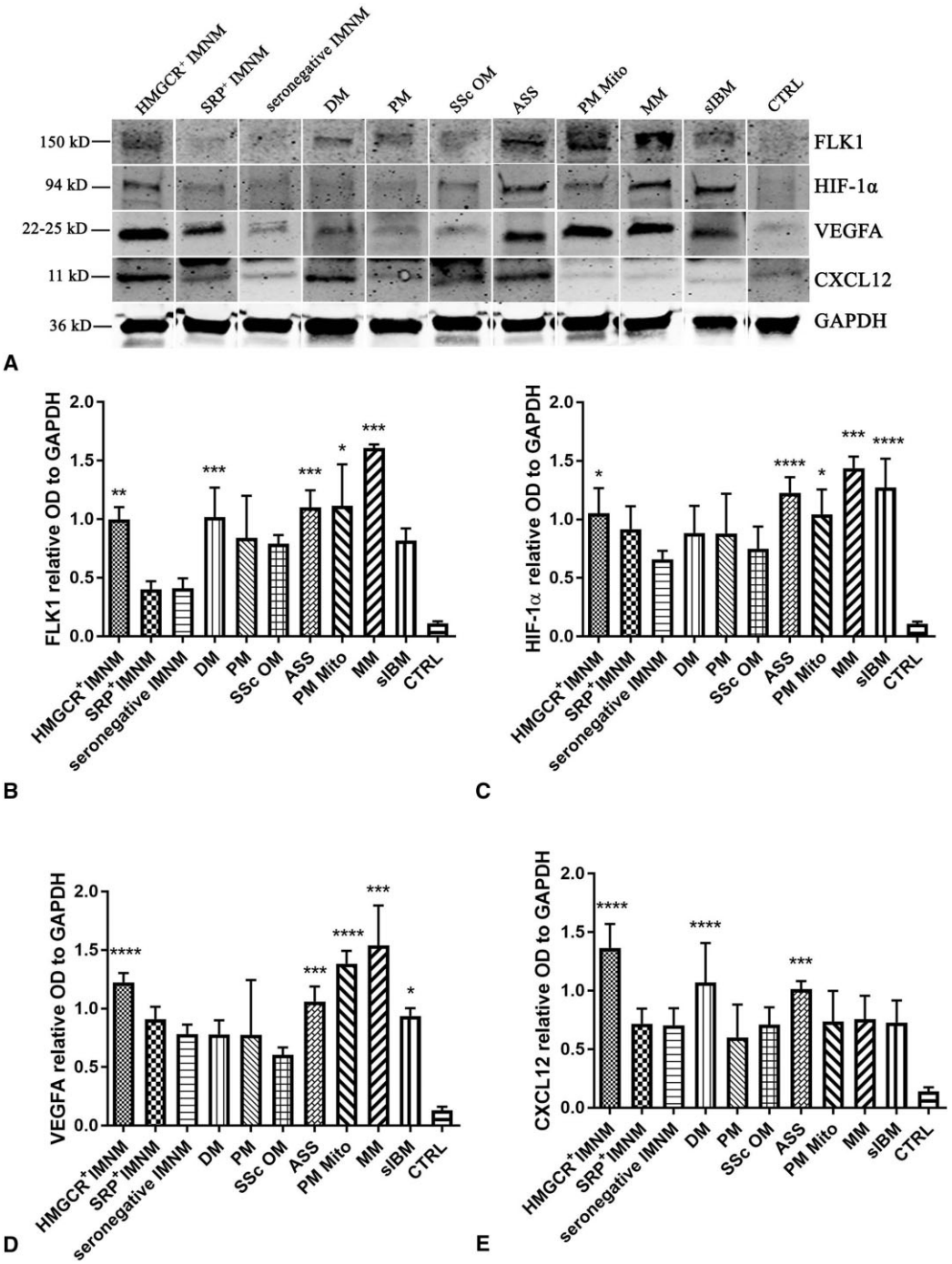

Western blot analysis of FLK1, HIF-1α, VEGF-A and CXCL12 expression in muscle biopsies of IIMs affected patients reveals a significantly higher level of these proteins in anti-HMGCR$^+$ IMNM than controls (**A**–**E**). In detail, the VEGF-A receptor FLK1 is significantly overexpressed in anti-HMGCR$^+$ IMNM, DM, ASS, PM-Mito, and MM compared with controls (**A**, **B**). The transcription factor HIF-1α is significantly increased in anti-HMGCR$^+$ IMNM, ASS, PM-Mito, MM, and sporadic IBM compared with controls (**A**, **C**). The pro-angiogenic factor VEGF-A is significantly upregulated in anti-HMGCR$^+$ IMNM, ASS, PM-Mito, MM, and sporadic IBM compared with controls (**A**, **D**). The chemokine CXCL12 is significantly upregulated in anti-HMGCR$^+$ IMNM, DM, and ASS compared with controls (**A**, **E**). The cropped bands represent independent experiments in duplicate for each protein; GAPDH was used as the internal control. Data are expressed as proteins/GAPDH ratio (S.D.). One-way ANOVA test with Dunnet's correction was applied. *$P<0.05$, **$P<0.01$, ***$P<0.001$, ****$P<0.0001$ for comparison with CTRL. IMNM: immune-mediated necrotizing myopathy.

myopathy [35]. Further studies need to be carried out to explain the observed mismatch between CD and angiogenic factors in anti-Jo1$^+$ ASS myopathy. In anti-HMGCR$^+$ IMNM, despite the weak HIF-1α- and VEGF-A staining detectable on myofibres and blood vessels, the WB analysis showed an increment of these two angiogenic molecules. Consequently, FLK1 appeared overexpressed by endomysial capillaries in response to VEGF-A mainly released by macrophages. Additional angiogenic stimuli can coexist and involve different cytotypes. Nevertheless, the macrophages seem to produce a greater extent of molecules and their co-expression of CXCL12 and VEGF-A could confer a particular strength to the synchronized vasculomyogenesis [21, 22]. In fact, both these angiogenic molecules have been related to muscle regeneration and angiogenesis [22, 36, 37], together with HIF-1α [38]. Macrophages are important for tissue healing, they express VEGF [39] or CXCL12 [(23)] or both angiogenic factors together [40], and M2 macrophages may express even higher levels of VEGF and CXCL12 than the M1 subpopulation [40]. Macrophages are the predominant inflammatory cells in IMNM [1, 10, 11, 13, 24, 41] and have been specifically characterized in their alternative activation states in IMNM biopsies, M1 pro-inflammatory [1, 13] or M2 regenerative macrophages [10]. In our study, we showed that both M1 and M2 macrophage densities were significantly higher in anti-HMGCR$^+$ IMNM than in the other IIMs. Yet, a very considerable proportion of the M2 macrophages expressed VEGF-A and CXCL12 and the density of M2 VEGF-A$^+$/arginase-1$^+$ macrophages and their proportion were significantly higher in anti-HMGCR$^+$ than in anti-SRP$^+$ IMNM. Anti-SRP$^+$ myopathy is generally clinically and pathologically more severe than anti-HMGCR$^+$ IMNM [1, 7, 9]. Also in our study, the highest percentage of attacked myofibres with sarcolemmal complement staining was found in anti-SRP$^+$ IMNM, where lower levels of angiogenic macrophages and normal CD were measured, as previously demonstrated [28]. Thus, our findings on the M1/M2 macrophage density ratio suggest that in anti-HMGCR$^+$ IMNM, an early phenotype switch toward M2 differentiation is promoted, as observed in the experimental model of macrophage phagocytosis [42]. The transition of macrophages from the M1 to M2 phenotype probably accompanies muscle transition from the macrophage-driven promotion of satellite cells proliferation to their differentiation and subsequent muscle repair in several muscle models [43–46], through the increased levels of the M2 macrophage arginase-1.

The main limitation of this study is the small sample size, but inflammatory and non-inflammatory myopathies are notoriously rare conditions. Nevertheless, our study may add new insights into the role of macrophages in patients affected by different myopathies. A strength of our study is that all patients were untreated at the time of the muscle biopsy.

In summary, our study provides evidence that anti-HMGCR$^+$ IMNM features a unique pathotype characterized by a striking increase in CD and high numbers of perivascular M1 and M2 macrophages expressing angiogenic molecules. Furthermore, the density of M2 macrophages expressing VEGF-A was strongly correlated with angiogenesis, suggesting they may have a pivotal role in the regeneration of injured muscle tissue [47]. Differentiating myogenic cells require a supportive microenvironment by neighboring cells residing in the stem muscle niche, comprising activated microvessels, which supply oxygen, nutrients and prosurvival signals [48]. A coordinated effort by M1 shifting to M2 proangiogenic macrophages is required to support synchronized vasculomyogenesis through active interaction with endothelial cells and pericytes [49, 50]. The identification of specific molecules for modulating M1 pro-inflammatory macrophages might offer a therapeutic target for anti-HMGCR$^+$ IMNM patients.

Acknowledgements

The authors thank M.V.C. Pragnell, BA, for linguistic help; R. Tamma, PhD, for providing help with image acquisition of CD31-stained slides; F. Fumai and M. de Giorgis, Tech., for technical help in IHC. Investigation/Formal analyses: A.L., T.A., M.F., M.G., D.D'A., M.E., L.L., A.A., M.Ta., F.G. Writing – original draft preparation: L.A., T.A., M.F., F.G. Writing – review & editing: T.A., M.F., F.G. Resources: D.D'A., A.A., M.Ta. Conceptualization/Supervision/Project administration/Funding acquisition: M.Tr., D.V., D.R., L.S., F.I., F.G.

Funding: This work was supported by the Italian Ministry of Education, University and Research (MIUR, Finanziamento delle attività base di ricerca 2017; to F.G.), and intramural funding (to F.I. and M.Tr.).

Disclosure statement: The authors have declared no conflicts of interest.

Data availability statement

The data underlying this article are available in the article and in its online supplementary material.

Supplementary data

Supplementary data are available at *Rheumatology* online.

References

1 Allenbach Y, Arouche-Delaperche L, Preusse C *et al.* Necrosis in anti-SRP(+) and anti-HMGCR(+) myopathies: role of autoantibodies and complement. Neurology 2018; 90:e507–e17.

2 Hoogendijk JE, Amato AA, Lecky BR *et al.* 119th ENMC international workshop: trial design in adult idiopathic inflammatory myopathies, with the exception of

inclusion body myositis, 10-12 October 2003, Naarden, The Netherlands. Neuromuscul Disord 2004;14: 337–45.

3 Targoff IN, Johnson AE, Miller FW. Antibody to signal recognition particle in polymyositis. Arthritis Rheum 1990;33:1361–70.

4 Mammen AL, Chung T, Christopher-Stine L *et al.* Autoantibodies against 3-hydroxy-3-methylglutaryl-coenzyme A reductase in patients with statin-associated autoimmune myopathy. Arthritis Rheum 2011;63:713–21.

5 Christopher-Stine L, Casciola-Rosen LA, Hong G *et al.* Novel autoantibody recognizing 200-kd and 100-kd proteins is associated with an immune-mediated necrotizing myopathy. Arthritis Rheum 2010;62:2757–66.

6 Allenbach Y, Benveniste O, Stenzel W, Boyer O. Immune-mediated necrotizing myopathy: clinical features and pathogenesis. Nat Rev Rheumatol 2020;16:689–701.

7 Watanabe Y, Uruha A, Suzuki S *et al.* Clinical features and prognosis in anti-SRP and anti-HMGCR necrotising myopathy. J Neurol Neurosurg Psychiatry 2016;87: 1038–44.

8 Allenbach Y, Drouot L, Rigolet A *et al.* Anti-HMGCR autoantibodies in European patients with autoimmune necrotizing myopathies: inconstant exposure to statin. Medicine 2014;93:150–7.

9 Pinal-Fernandez I, Casal-Dominguez M, Carrino JA *et al.* Thigh muscle MRI in immune-mediated necrotising myopathy: extensive oedema, early muscle damage and role of anti-SRP autoantibodies as a marker of severity. Ann Rheum Dis 2017;76:681–7.

10 Chung T, Christopher-Stine L, Paik JJ, Corse A, Mammen AL. The composition of cellular infiltrates in anti-HMG-CoA reductase-associated myopathy. Muscle Nerve 2015;52:189–95.

11 Allenbach Y, Mammen AL, Benveniste O, Stenzel W; Immune-Mediated Necrotizing Myopathies Working Group. 224th ENMC International Workshop: clinico-sero-pathological classification of immune-mediated necrotizing myopathies Zandvoort, The Netherlands, 14-16 October 2016. Neuromuscul Disord 2018;28:87–99.

12 Stenzel W, Goebel HH, Aronica E. Review: immune-mediated necrotizing myopathies–a heterogeneous group of diseases with specific myopathological features. Neuropathol Appl Neurobiol 2012;38:632–46.

13 Preuße C, Goebel HH, Held J *et al.* Immune-mediated necrotizing myopathy is characterized by a specific Th1-M1 polarized immune profile. Am J Pathol 2012;181: 2161–71.

14 Zhang J, Muri J, Fitzgerald G *et al.* Endothelial lactate controls muscle regeneration from ischemia by inducing M2-like macrophage polarization. Cell Metab 2020;31: 1136–53.e7.

15 Zhang Y, Liu J, Zou T *et al.* DPSCs treated by TGF-beta1 regulate angiogenic sprouting of three-dimensionally co-cultured HUVECs and DPSCs through VEGF-Ang-Tie2 signaling. Stem Cell Res Ther 2021;12:281.

16 Dace DS, Khan AA, Kelly J, Apte RS. Interleukin-10 promotes pathological angiogenesis by regulating macrophage response to hypoxia during development. PLoS One 2008;3:e3381.

17 Grundtman C, Tham E, Ulfgren AK, Lundberg IE. Vascular endothelial growth factor is highly expressed in muscle tissue of patients with polymyositis and patients with dermatomyositis. Arthritis Rheum 2008;58:3224–38.

18 Volpi N, Pecorelli A, Lorenzoni P *et al.* Antiangiogenic VEGF isoform in inflammatory myopathies. Mediators Inflamm 2013;2013:219313.

19 Baumann M, Gumpold C, Mueller-Felber W *et al.* Pattern of myogenesis and vascular repair in early and advanced lesions of juvenile dermatomyositis. Neuromuscul Disord 2018;28:973–85.

20 Chai KX, Chen YQ, Fan PL, Yang J, Yuan X. STROBE: the correlation of Cyr61, CTGF, and VEGF with polymyositis/dermatomyositis. Medicine 2018;97:e11775.

21 Bobadilla M, Sainz N, Abizanda G *et al.* The CXCR4/SDF1 axis improves muscle regeneration through MMP-10 activity. Stem Cells Dev 2014;23:1417–27.

22 Hardy D, Fefeu M, Besnard A *et al.* Defective angiogenesis in CXCL12 mutant mice impairs skeletal muscle regeneration. Skelet Muscle 2019;9:25.

23 De Paepe B, Schroder JM, Martin JJ, Racz GZ, De Bleecker JL. Localization of the alpha-chemokine SDF-1 and its receptor CXCR4 in idiopathic inflammatory myopathies. Neuromuscul Disord 2004;14: 265–73.

24 Girolamo F, Lia A, Annese T *et al.* Autophagy markers LC3 and p62 accumulate in immune-mediated necrotizing myopathy. Muscle Nerve 2019;60:315–27.

25 Lahoria R, Selcen D, Engel AG. Microvascular alterations and the role of complement in dermatomyositis. Brain 2016;139:1891–903.

26 Emslie-Smith AM, Engel AG. Microvascular changes in early and advanced dermatomyositis: a quantitative study. Ann Neurol 1990;27:343–56.

27 Estruch R, Grau JM, Fernandez-Sola J *et al.* Microvascular changes in skeletal muscle in idiopathic inflammatory myopathy. Hum Pathol 1992;23:888–95.

28 Miller T, Al-Lozi MT, Lopate G, Pestronk A. Myopathy with antibodies to the signal recognition particle: clinical and pathological features. J Neurol Neurosurg Psychiatry 2002;73:420–8.

29 Corallo C, Cutolo M, Volpi N *et al.* Histopathological findings in systemic sclerosis-related myopathy: fibrosis and microangiopathy with lack of cellular inflammation. Ther Adv Musculoskelet Dis 2017;9:3–10.

30 Konttinen YT, Mackiewicz Z, Povilenaite D *et al.* Disease-associated increased HIF-1, alphavbeta3 integrin, and Flt-1 do not suffice to compensate the damage-inducing loss of blood vessels in inflammatory myopathies. Rheumatol Int 2004;24:333–9.

31 Carry MR, Ringel SP, Starcevich JM. Distribution of capillaries in normal and diseased human skeletal muscle. Muscle Nerve 1986;9:445–54.

32 Banker BQ. Dermatomyostis of childhood, ultrastructural alteratious of muscle and intramuscular blood vessels. J Neuropathol Exp Neurol 1975;34:46–75.

33 Taivassalo T, Ayyad K, Haller RG. Increased capillaries in mitochondrial myopathy: implications for the regulation of oxygen delivery. Brain 2012;135:53–61.

34 Wienke J, Mertens JS, Garcia S *et al.* Biomarker profiles of endothelial activation and dysfunction in rare systemic autoimmune diseases: implications for cardiovascular risk. Rheumatology 2021;60:785–801.

35 Williams TF, Mirando AC, Wilkinson B, Francklyn CS, Lounsbury KM. Secreted Threonyl-tRNA synthetase stimulates endothelial cell migration and angiogenesis. Sci Rep 2013;3:1317.

36 Brzoska E, Kowalewska M, Markowska-Zagrajek A *et al.* Sdf-1 (CXCL12) improves skeletal muscle regeneration via the mobilisation of Cxcr4 and CD34 expressing cells. Biol Cell 2012;104:722–37.

37 Beckman SA, Chen WC, Tang Y *et al.* Beneficial effect of mechanical stimulation on the regenerative potential of muscle-derived stem cells is lost by inhibiting vascular endothelial growth factor. Arterioscler Thromb Vasc Biol 2013;33:2004–12.

38 Flisiński M, Brymora A, Bartłomiejczyk I *et al.* Decreased hypoxia-inducible factor-1alpha in gastrocnemius muscle in rats with chronic kidney disease. Kidney Blood Press Res 2012;35:608–18.

39 Colegio OR, Chu NQ, Szabo AL *et al.* Functional polarization of tumour-associated macrophages by tumour-derived lactic acid. Nature 2014;513:559–63.

40 Wang Y, Chang T, Wu T *et al.* M2 macrophages promote vasculogenesis during retinal neovascularization by regulating bone marrow-derived cells via SDF-1/VEGF. Cell Tissue Res 2020;380:469–86.

41 Fornaro M, Girolamo F, Cavagna L *et al.* Severe muscle damage with myofiber necrosis and macrophage infiltrates characterize anti-Mi2 positive dermatomyositis. Rheumatology 2021;60:2916–26.

42 Fadok VA, Bratton DL, Konowal A *et al.* Macrophages that have ingested apoptotic cells in vitro inhibit proinflammatory cytokine production through autocrine/paracrine mechanisms involving TGF-beta, PGE2, and PAF. J Clin Invest 1998;101:890–8.

43 Tidball JG. Mechanisms of muscle injury, repair, and regeneration. Compr Physiol 2011;1:2029–62.

44 Kharraz Y, Guerra J, Mann CJ, Serrano AL, Muñoz-Cánoves P. Macrophage plasticity and the role of inflammation in skeletal muscle repair. Mediators Inflamm 2013;2013:491497.

45 Nie M, Liu J, Yang Q *et al.* MicroRNA-155 facilitates skeletal muscle regeneration by balancing pro- and anti-inflammatory macrophages. Cell Death Dis 2016;7:e2261.

46 Sakaguchi S, Shono J, Suzuki T *et al.* Implication of anti-inflammatory macrophages in regenerative moto-neuritogenesis: promotion of myoblast migration and neural chemorepellent semaphorin 3A expression in injured muscle. Int J Biochem Cell Biol 2014;54:272–85.

47 Morosetti R, Mirabella M, Gliubizzi C *et al.* MyoD expression restores defective myogenic differentiation of human mesoangioblasts from inclusion-body myositis muscle. Proc Natl Acad Sci USA 2006;103:16995–7000.

48 Christov C, Chretien F, Abou-Khalil R *et al.* Muscle satellite cells and endothelial cells: close neighbors and privileged partners. Mol Biol Cell 2007;18:1397–409.

49 Dort J, Fabre P, Molina T, Dumont NA. Macrophages are key regulators of stem cells during skeletal muscle regeneration and diseases. Stem Cells Int 2019;2019:4761427.

50 Lescaudron L, Peltekian E, Fontaine-Perus J *et al.* Blood borne macrophages are essential for the triggering of muscle regeneration following muscle transplant. Neuromuscul Disord 1999;9:72–80.